REFINED MIXED METHOD FINITE ELEMENTS FOR SHELLS OF REVOLUTION

Phillip L. Gould[*]
Subir K. Sen[**]

Washington University, St. Louis, Mo.

A rotational shell finite element with mixed stress and displacement variables is derived for the case of arbitrary static loading. Accurate representation of the shell geometry together with high-order approximations for the dependent variables are combined to formulate a comparatively precise element containing only the basic number of degrees of freedom. Representative examples are used to study the convergence of the element and to provide a basis of comparison with a similar displacement-type element.

[*]   Associate Professor of Civil and Environmental Engineering
[**] Graduate Student, Civil and Environmental Engineering Department

INTRODUCTION

Finite elements for which the explicit nodal variables are a mixed set of stress and displacement terms have generally been derived from some form of the Hellinger-Reissner variational principle (1,2). For plate and shell problems, the mixed formulation appears to offer some significant advantages compared to the more conventional displacement approach (3). In the computation of moments,which are important design parameters, the advantage is quite obvious. In the mixed method the stress terms representing the moment resultants are determined directly as nodal variables, whereas in the displacement formulation they are computed by differentiating the approximate displacement functions and applying the constitutive relations. The mixed method therefore not only yields moments which are continuous over the inter-element boundary but also avoids the error usually introduced by differentiating the approximating functions. On the other hand, mixed-type elements usually have more nodal variables than displacement-type elements, but the difference is not large especially if transverse shear effects are included in both formulations.

The evolution of mixed-type finite elements for plates and shells has followed a somewhat similar pattern to that of displacement-type elements beginning with triangular plate bending elements with linear and constant moment and linear displacement functions (3,4) followed by the extension to linear moment and parabolic displacement fields (5). A generalization of the plate bending element to include vibration and instability problems has been noted (6). Just as in the displacement method, the first mixed formulation for shells utilized combined plane stress-plate bending flat elements to approximate the curved surface (7). Mixed-type triangular curved elements based on shallow shell theory using polynomial approximations of various degrees (8,9,10,11) and on non-shallow shell theory (8) have been proposed. Also, non-linear shallow shell elements have been described (8,11). However, in contrast to the pattern of development for the displacement-type elements the mixed-type axisymmetric shell element has received only limited attention to date (12).

It is apparent that axisymmetric problems can be treated using the general shell elements, but the inherent computational advantages provided by harmonic decoupling and a strongly banded set of algebraic equations make the use of specialized rotational shell elements attractive for a large class of problems. Accordingly, the objectives of this study are to derive and test a mixed-type curved element for a thin elastic shell of revolution under arbitrary static loading. Following an approach implemented for a displacement-type element (13,14), accurate geometric data will be utilized to the fullest extent and high-order polynomial approximations will be employed when necessary to achieve a comparatively precise solution with relatively few elements.

GEOMETRY

The geometry of the shell element is shown in Fig. 1. The equation of the meridian curve, $R = R(Z)$ is used to express the principal meridional radius of curvature R_φ as a function of the vertical coordinate Z

$$R_\varphi = -\frac{[1 + (R')^2]^{3/2}}{R''} \tag{1}$$

in which φ is the meridional curvilinear coordinate. In Eq. 1 the symbol $(\ )' = d(\ )/dZ$. The arc length for element i between nodes i and i+1, is

$$L_i = \int_{Z_i}^{Z_{i+1}} [1 + (R')^2]^{1/2} \, dZ \tag{2}$$

from which the nondimensional arc length variable

$$s = S/L_i \quad (o \leq s \leq 1) \tag{3}$$

is defined.

In the following derivation, it is necessary to evaluate numerous integrals which contain various combinations of the geometrical parameters R_φ and R. This is conveniently accomplished by representing each of these terms by a fourth-order Lagrangian interpolation polynomial in the variable s and then evaluating the subsequent integrals in closed form (13,15).

For closed shells of revolution with $\varphi = 0$ at the pole Eqs. 1 and 2 cannot be applied at the pole since $R' \rightarrow \infty$. A coordinate transformation for the cap element enables R_φ and L_i to be evaluated (15).

FINITE ELEMENT DERIVATION

Definition of Variables

For shells of revolution, it is convenient to take all variables in Fourier series form, to obtain the solution for each harmonic and then to combine the contributions of each harmonic by superposition. Accordingly, the displacements and rotations are taken as

$$\{D\} = \{D_f \mid D_c\} = \{U \ V \ W \mid B_\varphi \ B_\theta\} = \sum_{j=o}^{\infty} \lceil \Theta_1 \rfloor \{D^{(j)}(s)\} \tag{4a}$$

in which

$$\lceil \Theta_1 \rfloor = \lceil \cos j\theta \ \sin j\theta \ \cos j\theta \ \cos j\theta \ \sin j\theta \rfloor \tag{4b}$$

and

$$\{D^{(j)}(s)\} = \{D_f^{(j)} \mid D_c^{(j)}\} = \{u^{(j)} \ v^{(j)} \ w^{(j)} \mid \beta_\varphi^{(j)} \ \beta_\theta^{(j)}\} \tag{4c}$$
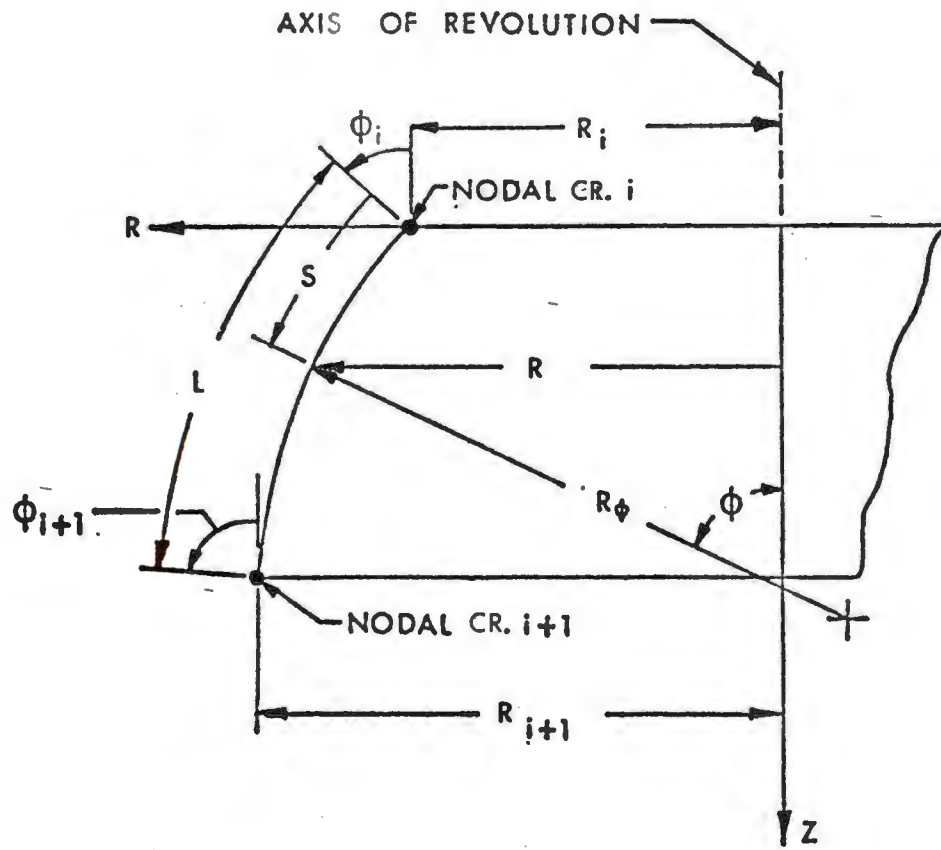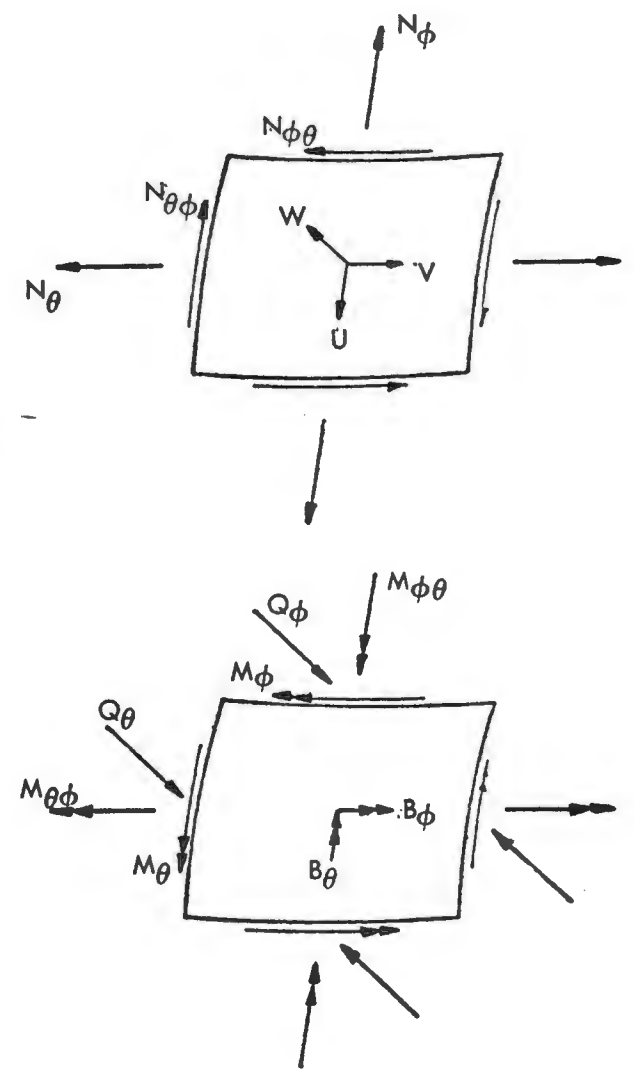
400

FIGURE 1 FINITE ELEMENT GEOMETRY

FIGURE 2 SIGN CONVENTION

In Eq. 4, U, V and W = the meridional, circumferential and normal displacements; β_φ and β_θ = the meridional and circumferential rotations, positive as shown in Fig. 2; and θ = the circumferential coordinate.

The strains and changes in curvature are taken as

$$\{H\} = \{H_f \mid H_c\} = \{E_\varphi\ E_{\varphi\theta}\ \Gamma_\varphi\ E_\theta\ E_{\theta\varphi}\ \Gamma_\theta \mid K_\varphi\ K_{\varphi\theta}\ K_\theta\ K_{\theta\varphi}\}$$

$$= \sum_{j=o}^{\infty} \lceil \Theta_2 \rfloor \{H^{(j)}(s)\} \tag{5a}$$

in which

$$\lceil \Theta_2 \rfloor = \lceil \cos j\theta\ \sin j\theta\ \cos j\theta\ \cos j\theta\ \sin j\theta\ \sin j\theta\ \cos j\theta\ \sin j\theta\ \cos j\theta\ \sin j\theta \rfloor \tag{5b}$$

and

$$\{H^{(j)}(s)\} = \{H_{f\varphi}^{(j)} \mid H_{f\theta}^{(j)} \mid H_{c\varphi}^{(j)} \mid H_{c\theta}^{(j)}\}$$

$$= \{\epsilon_\varphi^{(j)} \epsilon_{\varphi\theta}^{(j)} \gamma_\varphi^{(j)} \mid \epsilon_\theta^{(j)} \epsilon_{\theta\varphi}^{(j)} \gamma_\theta^{(j)} \mid \varkappa_\varphi^{(j)} \varkappa_{\varphi\theta}^{(j)} \mid \varkappa_\theta^{(j)} \varkappa_{\theta\varphi}^{(j)}\} \tag{5c}$$

In Eq. 5, E_φ, E_θ and $E_{\theta\varphi}$ = the meridional, circumferential and in-plane shearing strains; Γ_φ and Γ_θ = the meridional and circumferential transverse shearing strains and K_φ, K_θ and $K_{\theta\varphi}$ = the meridional, circumferential and twisting changes in curvature. It is assumed that $E_{\varphi\theta} = E_{\theta\varphi}$ and $K_{\varphi\theta} = K_{\theta\varphi}$.

The stress resultants and moment resultants are taken as

$$\{T\} = \{T_f \mid T_c\} = \{N_\varphi\ N_{\varphi\theta}\ Q_\varphi\ N_\theta\ N_{\theta\varphi}\ Q_\theta \mid M_\varphi\ M_{\varphi\theta}\ M_\theta\ M_{\theta\varphi}\}$$

$$= \sum_{j=o}^{\infty} \lceil \Theta_2 \rfloor \{T^{(j)}(s)\} \tag{6a}$$

in which

$$\{T^{(j)}(s)\} = \{T_{f\varphi}^{(j)} \mid T_{f\theta}^{(j)} \mid T_{c\varphi}^{(j)} \mid T_{c\theta}^{(j)}\}$$

$$= \{n_\varphi^{(j)} n_{\varphi\theta}^{(j)} q_\varphi^{(j)} \mid n_\theta^{(j)} n_{\theta\varphi}^{(j)} q_\theta^{(j)} \mid m_\varphi^{(j)} m_{\varphi\theta}^{(j)} \mid m_\theta^{(j)} m_{\theta\varphi}^{(j)}\} \tag{6b}$$

In Eq. 6, N_φ, N_θ and $N_{\theta\varphi}$ = the meridional, circumferential and in-plane shearing stress resultants; Q_φ and Q_θ = the meridional and circumferential transverse shearing stress resultants; and M_φ, M_θ and $M_{\theta\varphi}$ = the meridional, circumferential and twisting moment resultants, positive as shown in Fig. 2. It is assumed that $N_{\varphi\theta} = N_{\theta\varphi}$ and $M_{\varphi\theta} = M_{\theta\varphi}$.

The surface loading is taken as

$$\{F\} = \{F_\varphi \ F_\theta \ F_n\} = \sum_{j=o}^{\infty} \lceil \Theta_3 \rfloor \{F^{(j)}(s)\} \tag{7a}$$

in which

$$\lceil \Theta_3 \rfloor = \lceil \cos j\theta \ \sin j\theta \ \cos j\theta \rfloor \tag{7b}$$

and

$$\{F^{(j)}(s)\} = \{f_\varphi^{(j)} \ f_\theta^{(j)} \ f_n^{(j)}\} \tag{7c}$$

In Eq. 7, F_φ, F_θ and F_n = the distributed surface loading corresponding to the positive directions of U, V and W, respectively, as shown in Fig. 2. Also admissible are circumferentially distributed line loads applied at nodal circles, $R = R_i$, in the form

$$\{F_i\} = \{F_{\varphi i} \ F_{\theta i} \ F_{n i}\} = \sum_{j=o}^{\infty} \lceil \Theta_3 \rfloor \{F_i^{(j)}\} \tag{8a}$$

in which

$$\{F_i^{(j)}\} = \{f_{\varphi i}^{(j)} \ f_{\theta i}^{(j)} \ f_{n i}^{(j)}\} \tag{8b}$$

No applied couples are considered.

With all dependent variables and loading terms defined in separated form, the remaining derivation will proceed for a typical harmonic $j \geq 1$. For harmonic $j = 0$, the treatment is somewhat simplified since all terms dependent on $\sin j\theta$ are dropped.

Variational Formulation

Reissner's general variational theorem specialized for thin shell theory (16) serves as a basis for the mixed method finite element formulation envisaged in the present study. The theorem states that with the translational and rotational strain components satisfying the appropriate strain-displacement relationships, the governing equations of thin shell theory can be derived as the Euler equations of the variational problem. Prato (9) obtained a contracted form of the general variational principle by identically satisfying the stress resultant-strain relationships

$$\{T_f\} = f_1(H_f) \tag{9}$$

the moment equilibrium equations

$$\{Q_\varphi \ Q_\theta\} = f_2(T_c) \tag{10}$$

403

and the boundary conditions

$$\{T_c\}_b = \{\overline{T}_c\}_b \quad \text{on stress boundary } \sigma \tag{11a}$$

and

$$\{D_f\}_b = \{\overline{D}_f\}_b \quad \text{on displacement boundary } \delta \tag{11b}$$

In Eq. 11, the subscript b indicates the boundary value and the bar indicates a prescribed value of the variable.

For a typical harmonic $j \geq 1$ of an isotropic thin elastic shell of revolution subdivided into n discrete elements, the contracted functional takes the form

$$I^{(j)}(s) = \pi \sum_{i=1}^{n} \left[\left\{ \int_{o}^{1} [W_M^{(j)} - W_B^{(j)} + U^{(j)} + q_\varphi^{(j)}(\gamma_\varphi^{(j)} - \beta_\varphi^{(j)}) + q_\theta^{(j)}(\gamma_\theta^{(j)} - \beta_\theta^{(j)})] R L_i ds \right. \right.$$

$$\left. \left. + \{F_i^{(j)}\}^T \{D_f^{(j)}\} R_i \right\} - \{\overline{T}_{f\varphi}^{(j)}\}_b^T \{D_f^{(j)}\}_b \overline{R}_\sigma + \{T_{c\varphi}^{(j)}\}_b^T \{\overline{D}_c^{(j)}\}_b \overline{R}_\delta \right] \tag{12a}$$

in which

$$W_M^{(j)} = \frac{Eh}{2(1-\mu^2)} \left[\epsilon_\varphi^{(j)2} + \epsilon_\theta^{(j)2} + 2\mu\, \epsilon_\varphi^{(j)} \epsilon_\theta^{(j)} + 2(1-\mu)\, \epsilon_{\theta\varphi}^{(j)2} \right] \tag{12b}$$

  = Membrane strain energy density.

$$W_B^{(j)} = \frac{6}{Eh^3} \left[m_\varphi^{(j)2} + m_\theta^{(j)2} - 2\mu\, m_\varphi^{(j)} m_\theta^{(j)} + 2(1+\mu) m_{\theta\varphi}^{(j)2} \right]$$

$$+ \frac{1+\mu}{\lambda Eh} \left[q_\varphi^{(j)2} + q_\theta^{(j)2} \right] \tag{12c}$$

  = Complementary strain energy density associated with bending and transverse shear deformation.

$$U^{(j)} = \{F^{(j)}(s)\}^T \{D_f^{(j)}\} \tag{12d}$$

  = Potential energy density of the applied distributed loading

and

$$\{\overline{T}_{f\varphi}^{(j)}\}_b, \{\overline{D}_c^{(j)}\}_b = \text{Prescribed values of the force stress resultants}$$
and rotations at the boundaries where the horizontal radius $R(Z) = \overline{R}_\sigma$ and $\overline{R}_\delta$, respectively.

Also in Eqs. 12(b) and 12(c), h = the shell thickness, E = Young's modulus, μ = Poisson's ratio and λ = the shearing stress shape factor, commonly taken as 5/6.

The strain and rotation terms contained in Eq. 12 can be expressed in terms of the displacements using the strain-displacement relationships. For harmonic j of a rotational shell, these relationships take the form (17)

$$\{H^{(j)}(s)\} = [A^{(j)}(s)]\,\{D^{(j)}(s)\} \tag{13a}$$

in which

$$[A^{(j)}(s)] = \begin{bmatrix}
\dfrac{1}{L_i}\dfrac{d(\ )}{ds} & 0 & \dfrac{1}{R_\varphi} & 0 & 0 \\[2ex]
-\dfrac{1}{2R} & \dfrac{1}{2L_i}\dfrac{d(\ )}{ds}-\dfrac{\cos\varphi}{2R} & 0 & 0 & 0 \\[2ex]
-\dfrac{1}{R_\varphi} & 0 & \dfrac{1}{L_i}\dfrac{d(\ )}{ds} & 1 & 0 \\[2ex]
\dfrac{\cos\varphi}{R} & \dfrac{1}{R} & \dfrac{\sin\varphi}{R} & 0 & 0 \\[2ex]
-\dfrac{1}{2R} & \dfrac{1}{2L_i}\dfrac{d(\ )}{ds}-\dfrac{\cos\varphi}{2R} & 0 & 0 & 0 \\[2ex]
0 & -\dfrac{\sin\varphi}{R} & -\dfrac{1}{R} & 0 & 1 \\[2ex]
0 & 0 & 0 & \dfrac{1}{L_i}\dfrac{d(\ )}{ds} & 0 \\[2ex]
0 & 0 & 0 & -\dfrac{1}{2R} & \dfrac{1}{2L_i}\dfrac{d(\ )}{ds}-\dfrac{\cos\varphi}{2R} \\[2ex]
0 & 0 & 0 & \dfrac{\cos\varphi}{R} & \dfrac{1}{R} \\[2ex]
0 & 0 & 0 & -\dfrac{1}{2R} & \dfrac{1}{2L_i}\dfrac{d(\ )}{ds}-\dfrac{\cos\varphi}{2R}
\end{bmatrix} \tag{13b}$$

As previously noted, the moment equilibrium equations, which take the form

$$q_\varphi^{(j)}(s) = \left[\frac{\cos\varphi}{R}\left(m_\varphi^{(j)}-m_\theta^{(j)}\right)+\frac{1}{L_i}\frac{dm_\varphi^{(j)}}{ds}+\frac{1}{R}m_{\theta\varphi}^{(j)}\right] \tag{14a}$$

$$q_\theta^{(j)}(s) = \left[\frac{2\cos\varphi}{R}m_{\theta\varphi}^{(j)}+\frac{1}{L_i}\frac{dm_{\theta\varphi}^{(j)}}{ds}-\frac{1}{R}m_\theta^{(j)}\right] \tag{14b}$$

for a rotational shell, are used to eliminate the transverse shear resultants from Eq. 12(a). Thus, the contracted form of Reissner's functional is expressible in terms of six dependent variables, three displacements $(u^{(j)}, v^{(j)}, w^{(j)})$, and three moment resultants $(m_\varphi^{(j)}, m_\theta^{(j)}, m_{\theta\varphi}^{(j)})$.

The solution for the dependent variables which will make the functional, Eq. 12(a), stationary will be assumed in the form of polynomial comparison functions. The functional contains only the first-order derivatives of the dependent variables; as such, it is sufficient that the functions have continuous first derivatives over the element domain and be continuous over the interelement boundaries (18,19). The natural boundary conditions provided by the last two terms of Eq. 12(a) require that the force stress resultants $\{\bar{T}_{f\varphi}^{(j)}\}_b$ and the rotations $\{\bar{D}_c^{(j)}\}_b$ be continuous across the interelement boundaries. This requirement, together with the continuity restrictions imposed on the dependent variables, cancel out these terms at all interior boundaries. Therefore, only the expressions along the exterior boundaries need be retained and any non-zero boundary values of the force stress resultants and/or the rotations may be specified through these terms. If the specified boundary quantities correspond to the explicit variables of the functional, the known value is directly used.

Approximations for Dependent Variables and Loading

The dependent variables are assumed in the following form over the element domain:

$$\{Y^{(j)}(s)\} = \{u^{(j)}\ v^{(j)}\ w^{(j)}\ m_\varphi^{(j)}\ m_\theta^{(j)}\ m_{\theta\varphi}^{(j)}\}$$

$$= \{y_1(s)\ y_2(s)\ y_3(s)\ y_4(s)\ y_5(s)\ y_6(s)\} \tag{15a}$$

in which

$$y_\ell(s) = (1-s)y_\ell(o) + s\ y_\ell(1) + s(1-s)\sum_{m=1}^{\bar{\ell}} y_{\ell m}\ s^{m-1} \quad (\ell=1,6) \tag{15b}$$

In Eq. 15, $y_\ell(s)$ = the ℓth element of vector $\{Y^{(j)}(s)\}$; the coefficients $y_\ell(o)$ and $y_\ell(1)$ = the nodal values of $y_\ell(s)$; $y_{\ell 1} \cdots y_{\ell\bar{\ell}}$ = coefficients of the higher-order terms; and $\bar{\ell}$ = indicator of the degree, $\bar{\ell}+1$, of each polynomial. It should be noted that the form of the polynomials specified in Eq. 15 allows a different order of approximation to be selected for each dependent variable, and that with the higher-order terms vanishing at the nodal circles, $s = 0$ and $s = 1$, the continuity of the variables across the nodes is maintained.

The load potential $U^{(j)}$ given in Eq. 12(d) is computed in a consistent manner for any arbitrary distribution of the surface loading (13,15). In the subsequent numerical analysis, the loading is assumed to be of the following form:

$$\{F^{(j)}(s)\} = \{f_1\ f_2\ f_3\} \tag{16a}$$

in which

$$f_\ell(s) = (1-s)\ f_\ell(o) + s\ f_\ell(1) \quad (\ell = 1,3) \tag{16b}$$

406

and $f_\ell(o)$ and $f_\ell(1)$ represent the nodal values of the distributed loading.

Approximate Solution of System

The polynomials representing $u^{(j)}$, $v^{(j)}$ and $w^{(j)}$ given in Eq. 15(b) are substituted into Eq. 13 to get the strain-displacement relationships in terms of the comparison functions. Next, Eqs. 13 and 14 together with Eqs. 15(b) and 16(b) are substituted into Eq. 12. Then, after interchanging the order of variation and summation, the stationary condition for $I^{(j)}$, $\delta I^{(j)} = 0$, reduces to the set of algebraic equations

$$\sum_{i=1}^{n} \int_{o}^{1} \frac{\partial I^{(j)}}{\partial y_\ell(o)} \, RL_i ds = 0 \qquad (\ell = 1,6) \qquad (17)$$

$$\sum_{i=1}^{n} \int_{o}^{1} \frac{\partial I^{(j)}}{\partial y_\ell(1)} \, RL_i ds = 0 \qquad (\ell = 1,6) \qquad (18)$$

and

$$\sum_{i=1}^{n} \int_{o}^{1} \frac{\partial I}{\partial y_{\ell m}} \, RL_i ds = 0 \qquad \begin{matrix} (\ell = 1,6) \\[4pt] (m = 1,\overline{\ell}) \end{matrix} \qquad (19)$$

Equations 17-19 may be combined into

$$\sum_{i=1}^{n} \left([M_i^{(j)}] \, \{\hat{Y}_i^{(j)}\} = \{\hat{F}_i^{(j)}\} + \{\tilde{F}_i^{(j)}\} \right) \qquad (20a)$$

in which

$$\{\hat{Y}_i^{(j)}\} = \{y_1(o) \; y_2'(o) \ldots y_6(o) \; y_1(1) \; y_2(1) \ldots y_6(1) \, | \, y_{11} \ldots y_{1\overline{1}} \, \ldots \ldots y_{6\overline{6}} \}$$

$$= \{\hat{Y}_{i1}^{(j)} \, | \, \hat{Y}_{i2}^{(j)} \} \qquad (20b)$$

= the vector of nodal variables and coefficients of higher-order terms

$$\{\hat{F}_i^{(j)}\} = \{\hat{f}_1(o) \; \hat{f}_2(o) \; \hat{f}_3(o) \; o \; o \; o \; \hat{f}_1(1) \; \hat{f}_2(1) \; \hat{f}_3(1) \; o \; o \; o \, |$$

$$\hat{f}_{11} \ldots \hat{f}_{1\overline{1}} \; \hat{f}_{21} \ldots \hat{f}_{2\overline{2}} \; \hat{f}_{31} \ldots \hat{f}_{3\overline{3}} \; 0 \; 0 \; 0 \}$$

$$= \{\hat{F}_{i1}^{(j)} \, | \, \hat{F}_{i2}^{(j)} \} \qquad (20c)$$

= the external distributed load vector corresponding to $\{\hat{Y}_i^{(j)}\}$

$$\{\tilde{F}_i^{(j)}\} = \{F_i^{(j)} \ o \ o \ o \ F_{i+1}^{(j)} \ o \ o \ o \ | \ 0\} = \{\tilde{F}_{i1}^{(j)} \ | \ 0\} \qquad (20d)$$

$$= \text{ the external line load vector corresponding to } \{\hat{Y}^{(j)}\}$$

and

$[M_i^{(j)}]$ = the coefficient matrix which will be termed the <u>mixed</u> matrix.

In Eqs. 20(c,d), the large 0 represents a null vector of suitable dimension.

It is convenient to apply static condensation to Eq. 20(a) to reduce the number of unknowns (20). Considering any element i and partitioning the mixed matrix to conform with Eq. 20(b),

$$[M_i^{(j)}] = \begin{bmatrix} M_{i11}^{(j)} & | & M_{i12}^{(j)} \\ \hline M_{i21}^{(j)} & | & M_{i22}^{(j)} \end{bmatrix} \qquad (21a)$$

and solving for $\hat{Y}_{i2}^{(j)}$ in terms of $Y_{i1}^{(j)}$,

$$\{\hat{Y}_{i2}^{(j)}\} = [M_{i22}^{(j)}]^{-1} \{\hat{F}_{i2}^{(j)} - M_{i21}^{(j)} \hat{Y}_{i1}^{(j)}\} \qquad (21b)$$

Eq. 20(a) reduces to

$$\sum_{i=1}^{n} \left([\hat{M}_i^{(j)}] \{\hat{Y}_{i1}^{(j)}\} = \{\hat{F}_{ei}^{(j)}\} \right) \qquad (22a)$$

in which

$$\left[\hat{M}_i^{(j)}\right] = [M_{i11}^{(j)} - M_{i12}^{(j)} M_{i22}^{(j)-1} M_{i21}^{(j)}] \qquad (22b)$$

$$= \text{ the element mixed matrix}$$

and

$$\left\{\hat{F}_{ei}^{(j)}\right\} = \{\tilde{F}_{i1}^{(j)} + \hat{F}_{i1}^{(j)} - M_{i12}^{(j)} M_{i22}^{(j)-1} \hat{F}_{i2}^{(j)}\} \qquad (22c)$$

$$= \text{ the vector giving the contribution of the loads acting on element i to the equivalent nodal forces at nodes i and i+1.}$$

If the meridian of the shell is continuous, the variables $y_\ell(1)$ for element i are equal to the variables $y_\ell(o)$ for element i+1 and Eq. 22(a) may be directly assembled into a symmetric banded global set of equations

$$[\hat{M}^{(j)}] \, \{\hat{Y}_1{}^{(j)}\} = \{\hat{F}_e{}^{(j)}\} \qquad\qquad (23)$$

If meridian discontinuities occur, appropriate coordinate transformations are required (13). The homogeneous boundary conditions for the displacements and the moment resultants are applied by eliminating the specified variables along with the corresponding rows and columns of the global mixed matrix $[\hat{M}^{(j)}]$ and rows of the load vector $\{\hat{F}_e{}^{(j)}\}$.

The preceding solution format is identical to the familiar direct stiffness method; however, the resulting system of equations differs in one respect. The global mixed matrix is not positive definite and the popular Choleski square root method cannot be used. Gaussian elimination was used for the numerical work in this study.

Once the global vector $\{Y_1{}^{(j)}\}$ is determined, the local vectors $\{\hat{Y}_{i1}{}^{(j)}\}$ can be easily computed and then the higher-order coefficients $\{Y_{i2}{}^{(j)}\}$ found from Eq. 21(b). Internodal values of the displacements and moment resultants are calculated from Eq. 15(b). After a single differentiation of the comparison functions, the transverse shear stress resultants are determined from Eqs. 14(a) and 14(b) and the in-plane stress resultants from Eqs. 13 and the constitutive law.

Precision of Approximate Solution

The polynomial comparison functions for the dependent variables, Eqs. 15, may be truncated at any desirable value of ℓ. The algebraic simplicity of low-order expansions is very attractive and previous studies using mixed-type triangular shell elements have shown that solutions employing linear displacement functions (7,9) together with constant (7) and linear (9) moment functions both converge with a sufficient number of elements. When higher-order approximations were used with the triangular mixed-type elements, improved convergence was obtained at the expense of a more complicated derivation and an increased number of degrees of freedom (10,11). In the present rotational shell formulation, however, the high-order terms are incorporated with little added complexity and no increase in the size of the element mixed matrix.

Since the moment and force resultants have a derivative relationship to the displacements, these quantities usually exhibit poorer convergence than the displacements. The use of comparatively fewer high-order elements in place of a larger number of low-order elements will improve the convergence of these important design variables and also reduce the required computer time and storage. In the following example problems, two measures of convergence will be studied: i) increasing the number of elements for a constant order of approximation; and, ii) increasing the order of approximation for a constant number of elements.

Another item of interest which will be examined subsequently is the comparative merits of the mixed-type rotational shell element as compared to a displacement-type element. An available high-precision rotational shell element (14,15) is quite similar in many respects to the present element and provides a basis to evaluate the relative performance of the two types of elements for a selected group of problems.

Computer Program

A Fortran IV Computer program was written to analyze the example problems. The average running time on an IBM 360-50 computer (fast core) was 4-8 secs. per element per harmonic for quartic comparison functions with a reduction of approximately 1 sec. per element when quadratic expansions were used. The problems were also solved using the displacement formulation outlined in Ref. 15 and the time required was about the same as in the case of the mixed method for the same order of expansions of the variables.

Edge-Loaded Cylindrical Shell

Figs. 3 and 4 show results obtained from the analysis of an edge-loaded cylindrical shell, a familiar test problem in the finite element literature (22,14). The convergence of the meridional moment and transverse shear resultants are examined in Fig. 3 as the degree of the comparison function is increased, and in Fig. 4 as the number of element divisions is increased. Although the displacements, not shown, converge with the case 1 element breakdown using quadratic polynomials, Fig. 3 indicates that the meridional moment and transverse shear require a cubic approximation to give accurate results. The discontinuity in the computed shear force resultant at the first node point away from the free edge (Z = 0.25 in) is shown in Fig. 3. This discontinuity is quite large for quadratic approximation but is practically eliminated with quartic expansion. With an increased number of elements near the loaded edge, Fig. 4 shows that quadratic approximations are adequate to achieve convergence on the meridional moment and transverse shear, as well as the normal displacement.

Results obtained from a refined displacement-type element (14) using the case 1 element subdivision are given in Table 1 and it is seen that with cubic and quartic approximations, the mixed method solutions exhibit improved convergence over corresponding displacement method solutions.

The present problem has also been studied with respect to different order of approximations for displacements and moments and indications are that uniform expansions for all of the variables provide superior convergence.

Hydrostatically-Loaded Cylindrical Shell

A hydrostatically-loaded cylindrical shell is examined in Fig. 5 where 14 evenly spaced elements with increasing order of approximation are employed in the analysis. In Table 2, the results are compared with the displacement method solution (15) for various order of polynomial expansions. It may be observed that even the linear functions give good results for the meridional moment using the mixed-type element; however, the transverse shear is somewhat unsatisfactory since this quantity is constant over each element domain for a cylindrical shell if the meridional moment is linear, as indicated by Eq. 14(a). The quadratic approximation gives very good convergence for the moment and the shear. For the range of expansions considered in Table 2, the displacement method solutions, in general, exhibited less satisfactory convergence than the mixed formulation and the nodal discontinuities of the moment and transverse shear force were more pronounced.
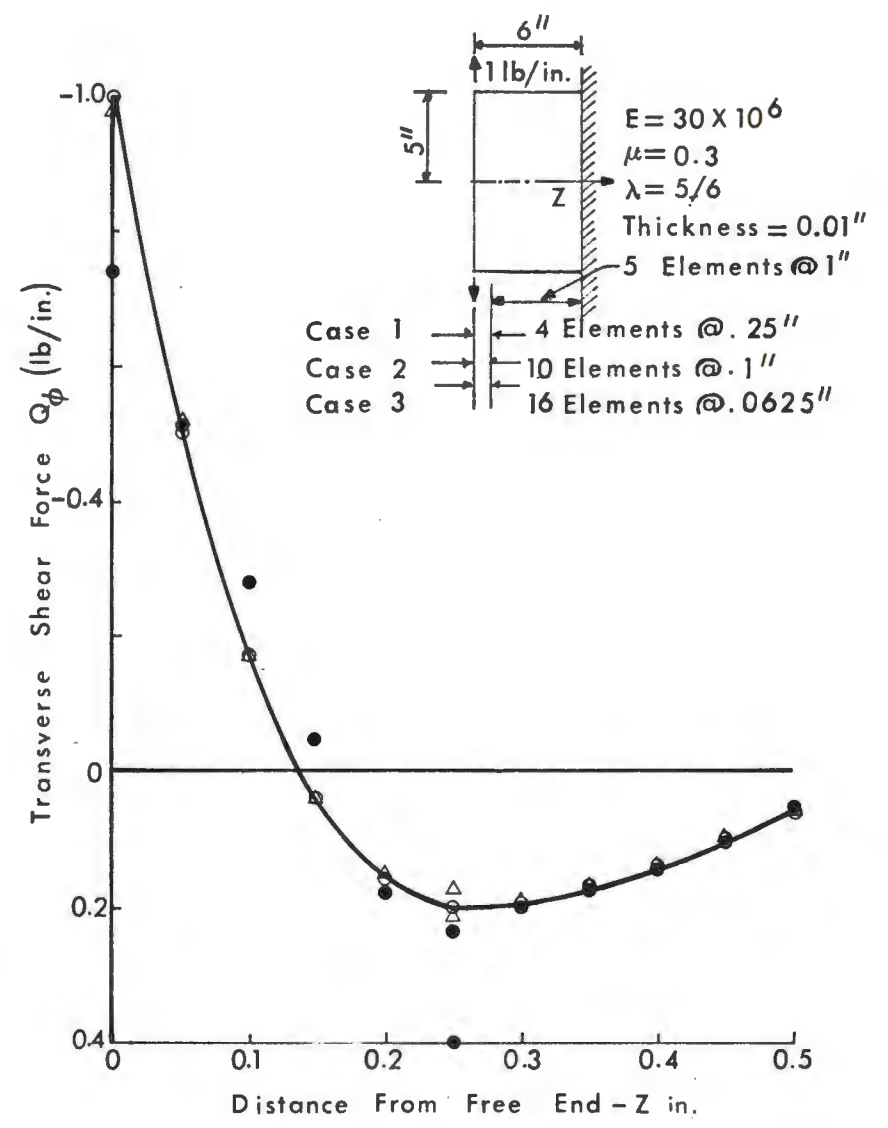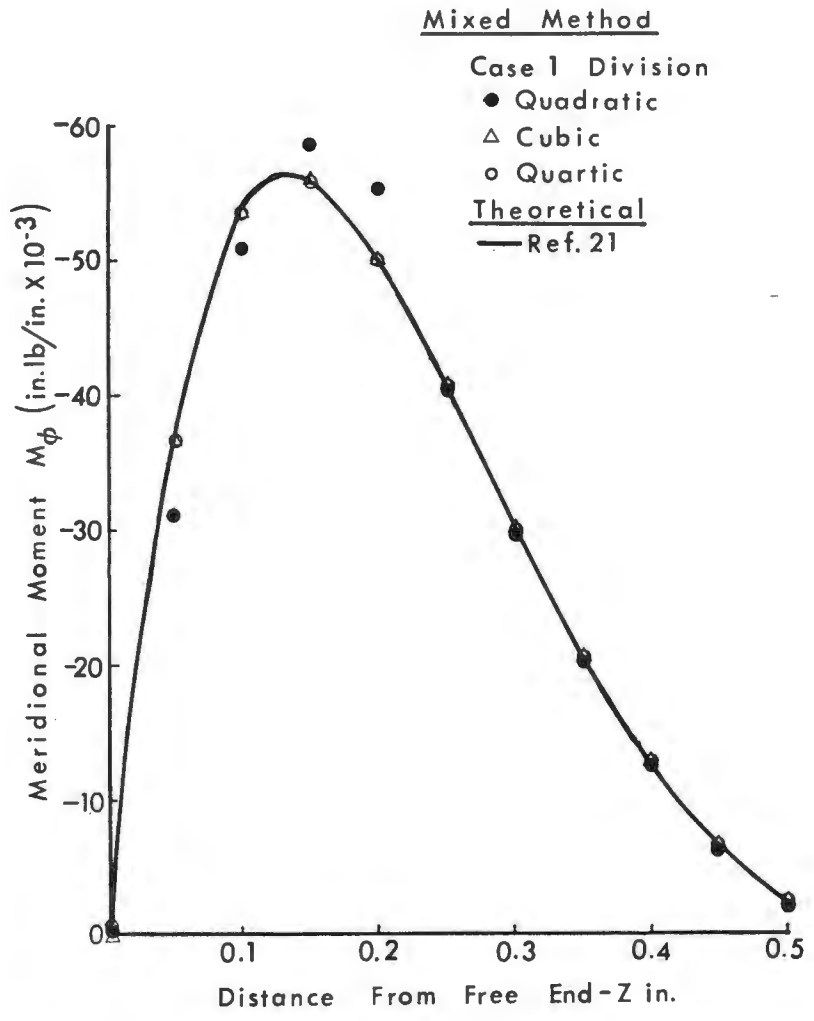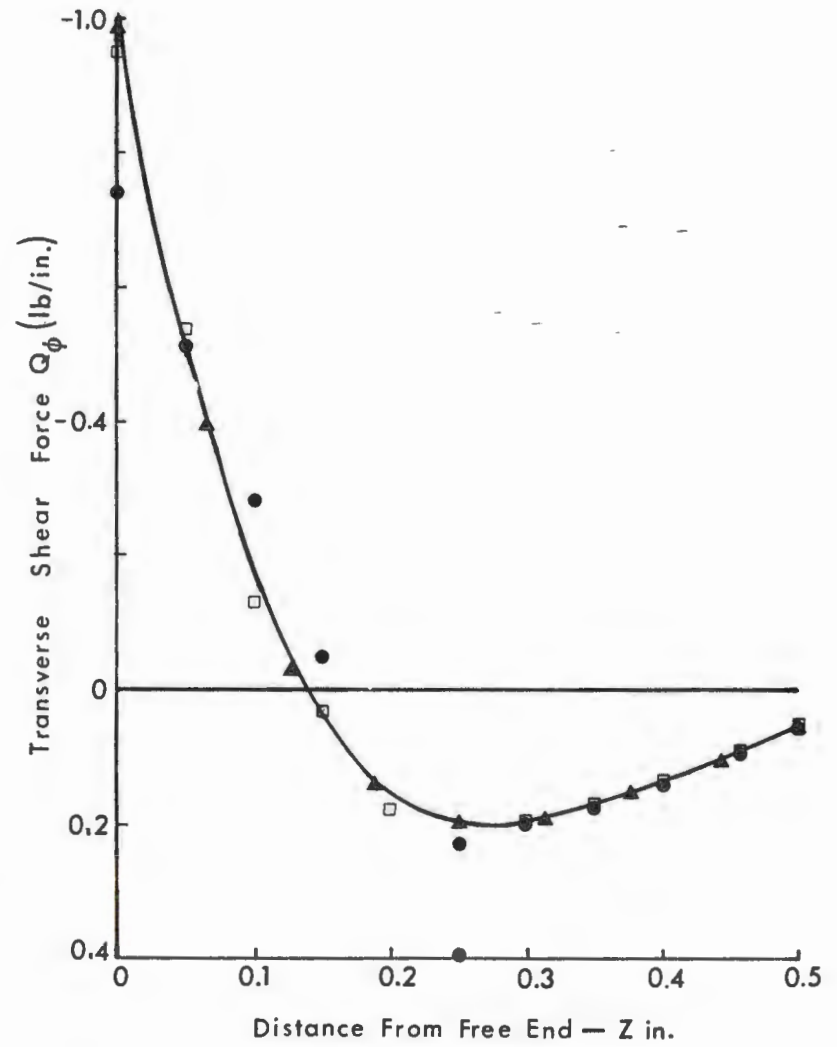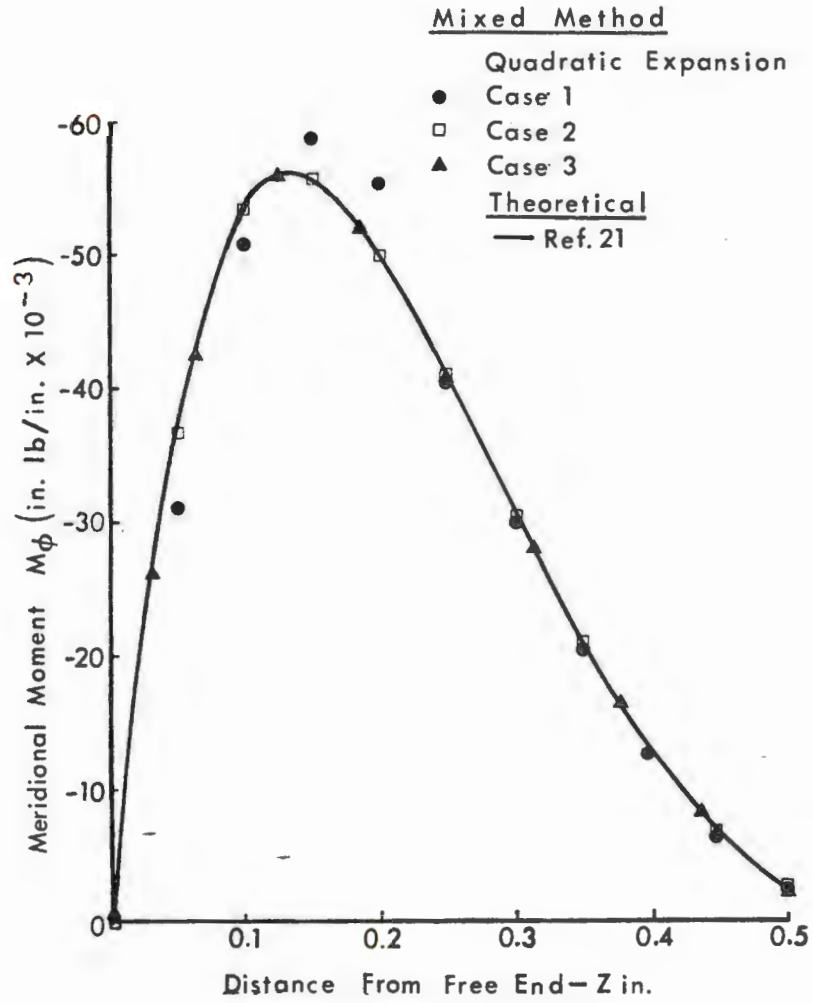
FIGURE 3. EDGE-LOADED CYLINDRICAL SHELL

FIGURE 4. EDGE-LOADED CYLINDRICAL SHELL

412

TABLE 1. Edge Loaded Cylindrical Shell (Case 1 Element Division)

| Dist. | Meridional Moment M_φ (in.lb/in x 10^{-3}) | | | | | Transverse Shear Force Q_φ (lb/in) | | | | |
| | Theoret. Results (Ref.21) | Displ. Finite Elem.[a] Order of Expansion | | Mixed Finite Elem. Order of Expansion | | Theoret. Results (Ref.21) | Displ. Finite Elem.[a] Order of Expansion | | Mixed Finite Elem. Order of Expansion | |
Z (in)		Cubic	Quartic	Cubic	Quartic		Cubic	Quartic	Cubic	Quartic
0.0	0.00	-28.50	- 5.82	0.00	0.00	-1.00	-2.24	-1.38	-0.97	-1.00
0.1	-53.23	-42.21	-51.84	-53.63	-53.22	-0.17	0.18	-0.25	-0.18	-0.17
0.2	-50.28	-53.14	-51.91	-50.06	-50.27	0.16	-0.28	0.32	0.17	0.16
0.3	-30.64	-29.98	-30.43	-30.55	-30.64	0.20	0.14	0.21	0.20	0.20
0.4	-13.02	-14.25	-13.15	-13.12	-13.01	0.14	0.19	0.14	0.15	0.14
0.5	- 2.59	- 1.09	- 2.44	- 2.61	- 2.61	0.07	0.14	0.07	0.07	0.07
0.6	1.67	1.05	1.59	1.67	1.66	0.02	0.03	0.03	0.02	0.02
0.7	2.40	2.58	2.49	2.37	2.39	-0.00	-0.12	-0.01	-0.00	-0.00
0.8	1.74	1.69	1.73	1.72	1.74	-0.01	-0.01	-0.01	-0.01	-0.01
0.9	0.88	0.93	0.92	0.87	0.88	-0.01	-0.01	-0.01	-0.01	-0.01
1.0	0.28	0.17	0.29	0.27	0.29	-0.00	-0.00	-0.00	-0.00	-0.00

a Results as per Ref. 15.

TABLE 2. Cylindrical Shell Under Hydrostatic Loading (14 Uniformly Spaced Elements)

| Dist. | Meridional Moment M_φ (in.lb/in x 10^3) | | | | | Transverse Shear Force Q_φ (lb/in x 10^2) | | | | |
| | Results as per Ref.15[b] | Displ. Finite Elem.[c] Order of Expansion | | Mixed Finite Elem. Order of Expansion | | Results as per Ref.15[b] | Displ. Finite Elem.[c] Order of Expansion | | Mixed Finite Elem. Order of Expansion | |
Z (in)		Quadratic	Cubic	Quadratic	Cubic		Quadratic	Cubic	Quadratic	Cubic
0.0	0.00	0.00	0.00	0.00	0.00	0.00	-0.01	0.00	0.00	0.00
89.1	- 0.04	- 0.05	- 0.05	- 0.04	- 0.04	0.04	0.07	0.04	0.04	0.04
133.7	0.46	0.45	0.46	0.46	0.46	0.20	0.34	0.30	0.20	0.20
178.2	1.80	1.81	1.80	1.80	1.80	0.39	0.65	0.39	0.40	0.39
200.5	2.68	2.71	2.69	2.68	2.68	0.38	0.63	0.39	0.39	0.38
222.8	3.34	3.40	3.35	3.34	3.34	0.17	0.27	0.18	0.20	0.17
245.1	3.17	3.27	3.19	3.17	3.17	-0.39	-0.68	-0.37	-0.35	-0.39
267.4	1.20	1.36	1.22	1.20	1.20	-1.47	-2.51	-1.45	-1.42	-1.47
289.7	- 3.87	- 3.68	- 3.84	- 3.87	- 3.87	-3.19	-5.41	-3.16	-3.14	-3.19
312.0	-13.47	-12.43	-13.43	-13.47	-13.47	-5.49	-8.43	-5.67	-5.46	-5.50

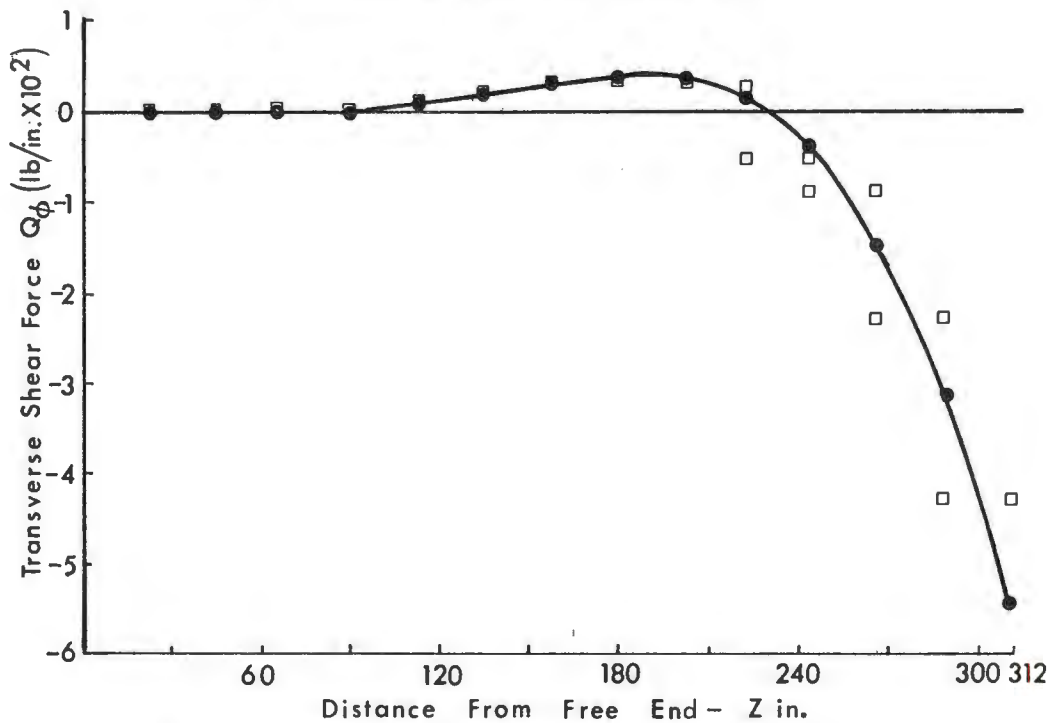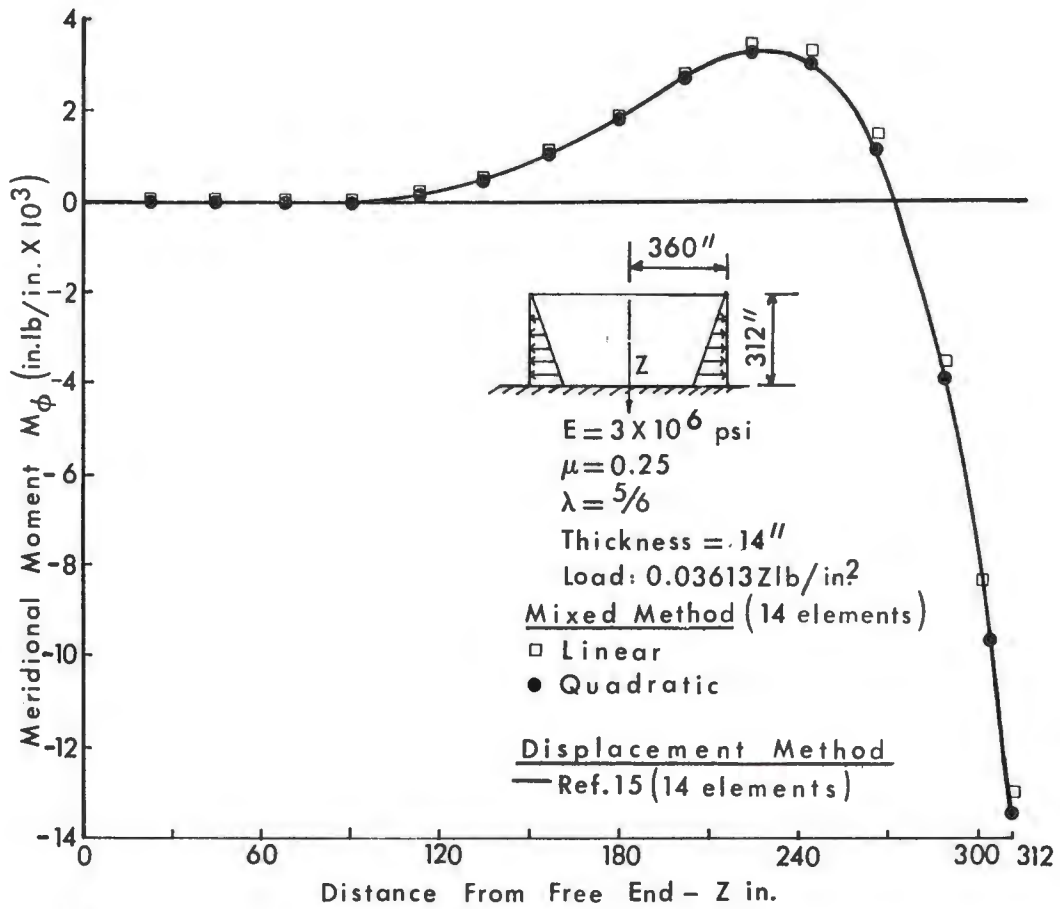b With sixth order expansions; c Results as per Ref. 15.

FIGURE 5 CYLINDRICAL SHELL UNDER HYDROSTATIC LOADING

414

This shell is moderately thick and the effect of shearing deformation is noticeable as the transverse shear and the meridional moment at the fixed end are approximately 3-4% lower than the corresponding values when the effect of shearing deformation is neglected (21).

Hyperboloidal Shell

A doubly curved shell of hyperboloidal shape subjected to an asymmetric loading is treated in Figs. 6 and 7. The shell is assumed to be fixed at the base. A quasistatic wind loading which is represented by the first 10 harmonics of the Fourier cosine expansion is considered (23). The meridional force and moment resultants obtained from the present formulation are compared with the results calculated by a displacement method solution with 200 conical-type elements (24). In Fig. 6, where 10 equally spaced elements are used (case 1 division), quartic expansions are required to find accurate moments near the base. For quadratic approximations of the variables, a 10 element idealization failed to predict the steep moment gradient in the vicinity of the base and a subsequent study with 20 equally spaced elements revealed that the computed moment at the base was 20% less than the actual value. However, when the number of elements near the base is increased (case 2 division), accurate results are obtained with quadratic approximations except for small inaccuracies in the meridional force near the free edge.

Results from a 10 element (case 1 division) displacement method solution (15) using quartic expansions are given in Table 3. Comparing these values with those obtained from Ref. 24, the meridional moments calculated using the displacement method are significantly less than the actual values near the base, while the moments found from the mixed solution are quite accurate. Both solutions yield comparatively accurate values for the meridional force.

SUMMARY AND CONCLUSIONS

A precise, mixed-type finite element analysis suitable for static analysis of shells of revolution has been presented. The formulation is based on a contracted form of Reissner's variational principle and includes the effect of transverse shear deformations. The shell element is in the form of a frustum of the meridional curve and fully incorporates the actual geometric data. The dependent variables in the formulation, the displacements and the moment resultants, have been represented by polynomial comparison functions which are continuous across the interelement boundaries and have continuous derivatives over the individual element domain. The continuity of the functions has been enforced by choosing the coefficients of the first-order terms to correspond to the nodal values of the variables and by forcing the higher-order terms to vanish at the nodal circles. The stationary condition of the functional yields a set of algebraic equations and static condensation permits the global mixed matrix to be expressed in terms of the nodal values of the variables alone, regardless of the order of the comparison functions.

The results of a number of test problems indicate that convergence can be achieved both by reducing the element size and by increasing the order of the comparison functions. However, from a computational standpoint, the use of high-order functions with fewer elements appears to be more efficient.
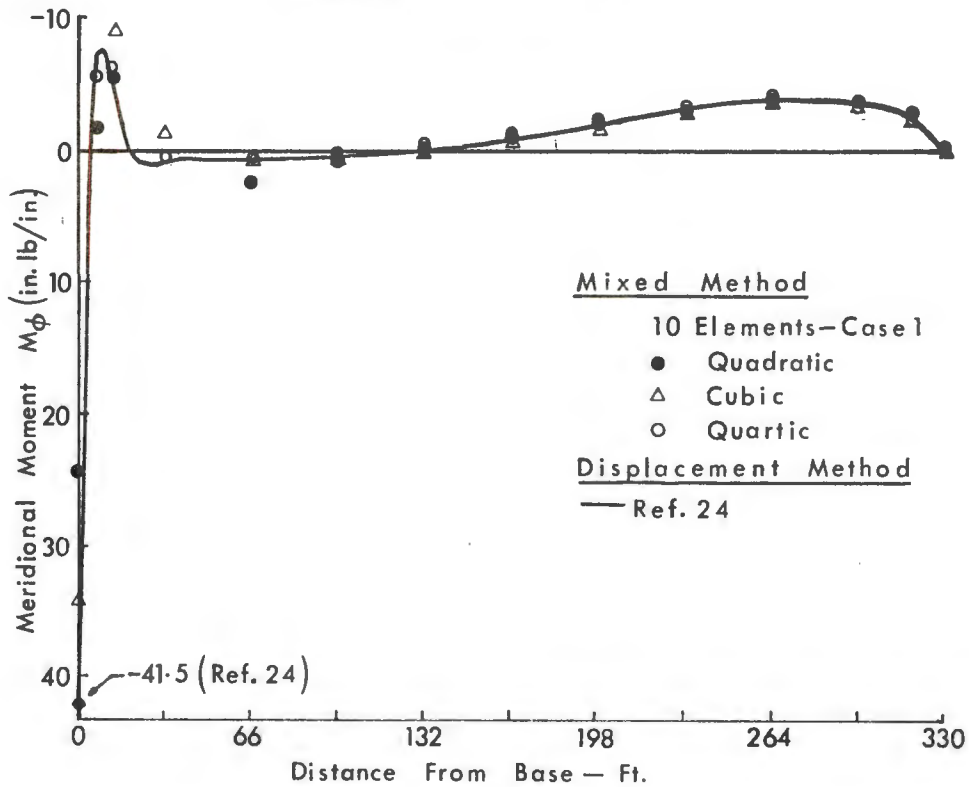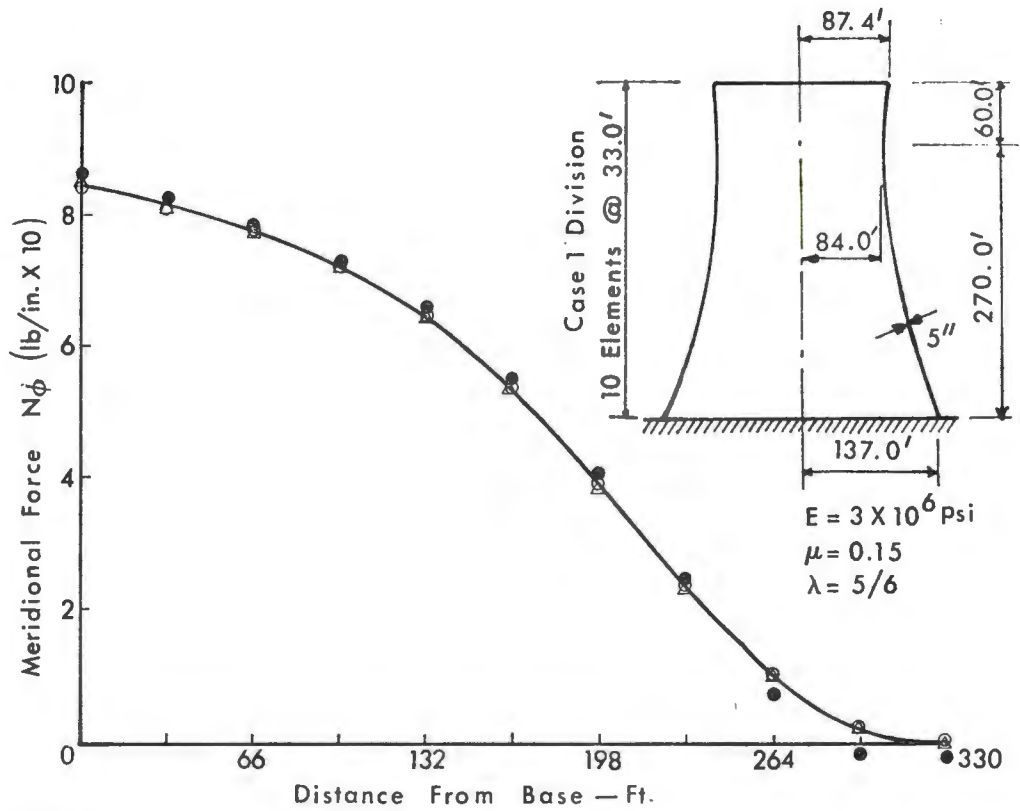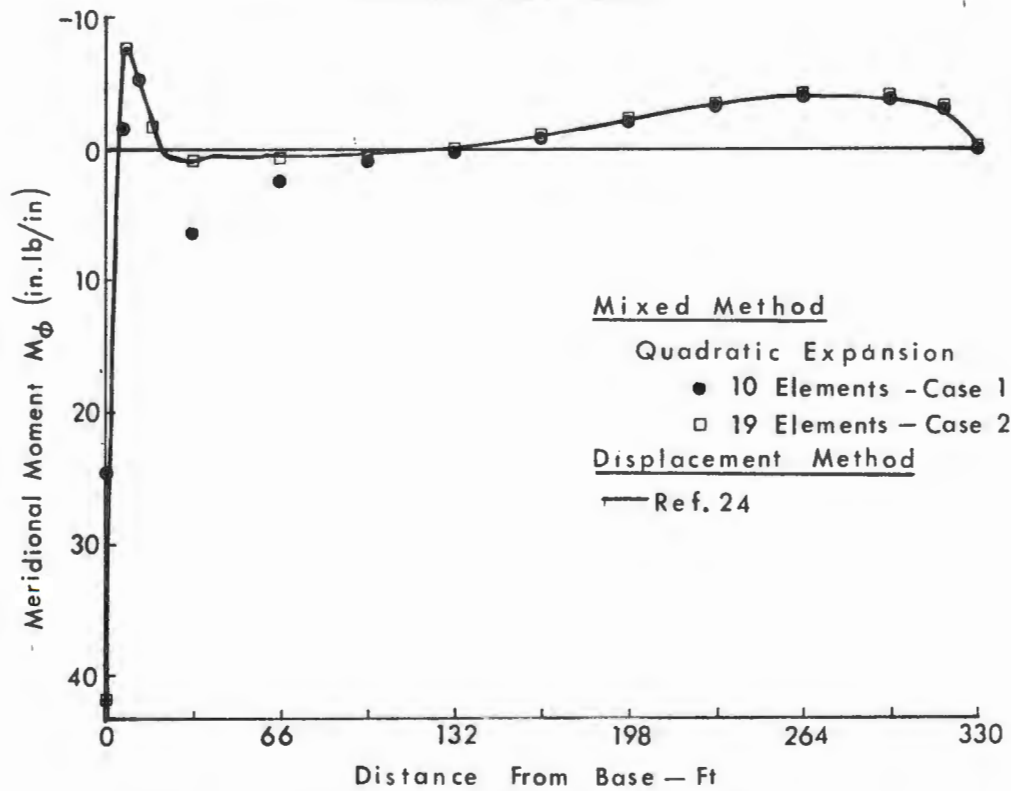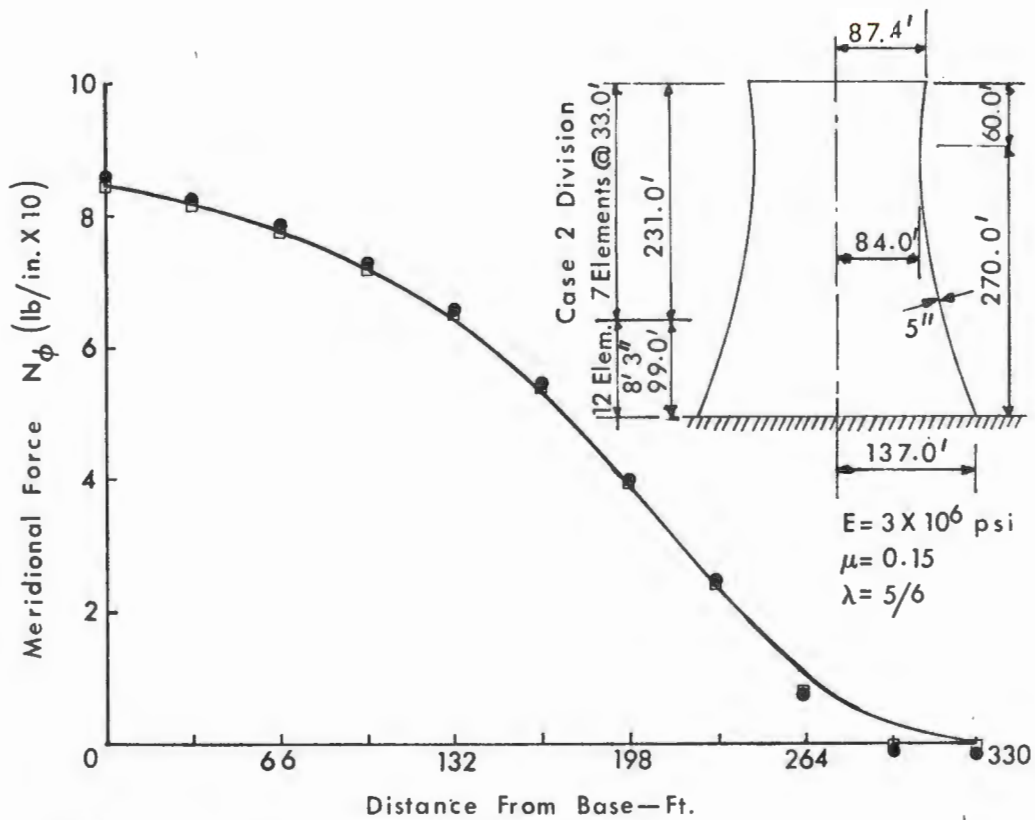
FIGURE 6 HYPERBOLOIDAL SHELL UNDER WIND LOAD

416

FIGURE 7 HYPERBOLOIDAL SHELL UNDER WIND LOAD

417

TABLE 3. Hyperboloidal Shell Under Wind Loading
(Quartic Expansion, 10 Elements)

Dist. from base (ft)	Meridional Moment M_φ (in. lb/in.)			Meridional Force N_φ (lb/in.)		
	Ref. 24[d]	Displ. Finite Elem.	Mixed Finite Elem.	Ref. 24[d]	Displ. Finite Elem.	Mixed Finite Elem.
0.0	41.50	18.02	41.98	84.30	84.22	84.35
6.6	- 6.20	3.22	- 5.78	83.60	84.02	83.91
13.2	- 5.40	- 4.52	- 6.22	83.30	83.08	83.15
19.8	- 0.30	- 5.40	1.46	82.60	82.51	82.58
26.4	0.90	0.36	1.26	82.00	82.25	82.15
33.0	0.60	5.39	0.30	81.00	81.25	81.20
66.0	0.60	0.46	0.64	77.30	77.78	77.68
99.0	0.40	0.43	0.43	72.60	72.45	72.32
132.0	0.00	- 0.08	- 0.08	64.40	64.73	64.51
165.0	- 0.90	- 0.86	- 0.88	53.50	53.76	53.42
198.0	- 2.00	- 1.92	- 1.98	39.10	39.62	39.08
231.0	- 3.50	- 3.17	- 3.28	24.10	24.29	23.49
264.0	- 4.40	- 4.10	- 4.11	11.10	11.18	10.28
297.0	- 4.40	- 3.62	- 3.93	2.80	2.92	2.34
330.0	0.00	0.05	0.00	0.00	0.00	0.02

d   Scaled values

418

Also, the results from the mixed method analysis were compared with those obtained from a displacement method solution using a similar type comparison function. It was observed that the mixed method solution exhibited improved accuracy over the displacement method solution for the same number of elements and the same order of expansion.

ACKNOWLEDGMENT

REFERENCES

1. Hellinger, E., "Die allgemeine Ansatz der Mechanik der Kontinua,"Art. 30, Encyklopädie Mathematischen Wissenschaften, mit Einschlus ihrer Anwendungen, Vol. 4, Part 4, Mechanik, 1914, pp. 601-694.

2. Reissner, E., "On a Variational Theorem in Elasticity," Journal of Mathematics and Physics, Vol. 29, 1950, pp. 90-95.

3. Herrmann, L. R., "A Bending Analysis for Plates," Proc. Conference on Matrix Methods in Structural Mechanics, AFFDL-TR-66-80, Wright Patterson Air Force Base, Ohio, 1965, pp. 577-604.

4. Herrmann, L. R., "Finite Element Bending Analysis for Plates," Journal of the Engineering Mechanics Division, ASCE, Vol. 93, No. EM5, Oct. 1967, pp. 13-26.

5. Visser, W., "A Refined Mixed-Type Plate Bending Element," AIAA Journal, Vol. 7, No. 9, Sept. 1969, pp. 1801-1803.

6. Cook, R. D., "Eigenvalue Problems with a'Mixed' Plate Element," AIAA Journal, Vol. 7, No. 5, May 1969, pp. 982-983.

7. Herrmann, L. R. and Campbell, D. M., "A Finite-Element Analysis for Thin Shells," AIAA Journal, Vol. 6, No. 10, Oct. 1968, pp. 1842-1847.

8. Prato, C. A., "A Mixed Finite Element Method for Thin Shell Analysis," Research Report R68-33, Dept. of Civil Engineering, Massachusetts Institute of Technology, 1968.

9. Prato, C. A., "Shell Finite Element Method Via Reissner's Principle," Int. J. Solids and Structures, Vol. 5, 1969, pp. 1119-1133.

10. Visser, W., "The Application of a Curved Mixed-Type Shell Element," IUTAM Symposium on High Speed Computing of Elastic Structures, Liege, Belgium, Aug. 1970.

11. Connor, J. and Will, D., "A Mixed Finite Element Shallow Shell Formulation," Proc. of the U.S.-Japan Seminar on Matrix Methods in Structural Analysis and Design, Tokyo, Sept. 1969, pp. 105-137.

12. Elias, Z. M., "Mixed Finite Element Method for Axisymmetric Shells," to be published in the International Journal for Numerical Methods in Engineering.

13. Brombolich, L. J. and Gould, P. L., "Finite Element Analysis of Shells of Revolution by Minimization of the Potential Energy Functional," Proc. of the Symposium on Application of Finite Element Methods in Civil Engineering, Vanderbilt University, Nashville, Tenn., 1969, pp. 279-307.

14. Brombolich, L. J. and Gould, P. L., "A High-Precision Curved Shell Finite Element," Proc. 12th Structures, Structural Dynamics and Materials Conf., AIAA and ASME, Anaheim, Calif., April, 1971.

15. Brombolich, L. J. and Gould, P. L., "High-Precision Finite Element Analysis of Shells of Revolution," Research Report No. 16, Structural Division, Dept. of Civil & Environmental Engineering, Washington University, St. Louis, Mo. 1970.

16. Reissner, E., "Variational Considerations for Elastic Beams and Shells," Journal of the Engineering Mechanics Division, ASCE, Vol. 88, No. EM1, Part I, Feb. 1962, pp. 23-57.

17. Washizu, K., "Variational Methods in Elasticity and Plasticity," Pergamon Press, 1968.

18. Strickland, J. A., "Geometrically Nonlinear Static and Dynamic Analysis of Shells of Revolution," IUTAM Symposium on High Speed Computing of Elastic Structures, Liege, Belgium, Aug. 1970.

19. Courant, R. and Hilbert, D., "Methods of Mathematical Physice," Vol. 1, Interscience, New York, 1953.

20. Przemieniecki, J. S., "Theory of Matrix Structural Analysis," McGraw-Hill Book Co., New York, 1968.

21. Timoshenko, S. and Woinowski-Krieger, S., Theory of Plates and Shells, 2nd Ed., McGraw-Hill Book Co., Inc., New York, 1959.

22. Grafton, P. E. and Strome, D. R. "Analysis of Axisymmetrical Shells by the Direct Stiffness Method," AIAA Journal, Vol. 1, No. 10, Oct. 1963, pp. 2342-2347.

23. Lee, S. L. and Gould, P. L., "Hyperbolic Cooling Towers under Wind Load," Journal of the Structural Division, ASCE, Vol. 93, No. ST5, Oct. 1967.

24. Hill, D. W. and Coffin, G. K., "Stresses and Deflections in Cooling Tower Shells Due to Wind Loading," Bulletin of the I.A.S.S., No. 35.